Analytic treatment of a driven oscillator with a limit cycle

E. J. Ding*
Institutt for Teoretisk Fysikk, Universitetet i Trondheim, N-7034 Trondheim-NTH, Norway
(Received 27 October 1986)

A prototype model of driven nonlinear oscillators with a stable limit cycle is studied. In the fast-relaxation limit, dynamics can be reduced to a one-dimensional mapping parametrized by the amplitude α and the phase β of the driving force. For a weak force, mode locking with rational winding numbers occurs. For a strong force, the parameter space may be divided into two subregions: In the unimodal region, the order of occurrence of the orbits is governed by the Metropolis-Stein-Stein U sequence of unimodal mappings; in the intermediate region, a transition between mode-locking behavior and that of the unimodal mapping takes place, and new sequences of periodic orbits occur. The systematics of the periodic orbits is investigated.

I. INTRODUCTION

Recent interest has focused on nonlinear oscillators driven by a periodic force, e.g., anharmonic oscillators,[1] a parametrically excited pendulum,[2] the forced Brusselator,[3,4] the Duffing's oscillator,[5] and so on.[6,7] Although a variety of physical systems have been modeled by different sets of equations, the resulting dynamics for large classes of systems display similar bifurcation and chaotic behavior. In particular, if the free oscillator has a stable limit cycle, enclosing an unstable stationary point, one often (not always, since it depends on the external force) finds, both in numerical simulations and in real experiments, that the parameter space has similar structure. For weak external force the limit cycle dominates, and mode-locking and quasiperiodic behaviors occur. With the external force increasing in amplitude, the oscillator passes through a complicated transition region where period-doubling sequences and chaotic behavior take place. For very strong external force, however, the oscillator is dominated by the driving force, and the chaotic behavior disappears. Great efforts have been made to reveal the fine structure of the parameter space, especially the transition between these two extreme situations. However, the results are so far incomplete. The reason is simple: The treatments are, in general, based on numerical solutions of the differential equations, and the structure of the transition is too complicated to be revealed by a direct integration of the equations of motion.

For a nonlinear driven oscillator with two variables, one may get a two-dimensional return map from the differential equations.[8] If the free oscillator can be solved exactly and is driven by impulse forces, the dynamics can be exactly reduced to a discrete mapping of two variables, which can be studied further by numerical methods.[6] In this paper the attention will be restricted to this simpler case. For other drives the dynamics becomes more complicated, and it will be discussed elsewhere.[9]

However, the model is still too complicated for a general discussion of the transition region between the weak- and the strong-force situations. I propose the following two steps to clarify the situation. (i) A prototype oscillator is chosen for simplicity. I claim that this oscillator contains the essential features of a wide class, and is thus representative. (ii) The limit of fast relaxation is taken, by which the dimension of the return map is reduced from $d=2$ to $d=1$, and a map from a circle onto itself (circle map[10]) results. Numerical experience shows that a finite relaxation rates gives results close to the limiting case.[9] With these two additional simplifications, the dynamics can be discussed in a fairly transparent manner, and one is, in particular, able to make the connection between a "devil's-staircase" region with mode-locking behavior[10] to a region with a unimodal mapping via a more complicated region of parameter space. In this intermediate region new sequences of periodic orbits occur.

The fast relaxation limit is technically important for the whole discussion in the present paper, since, as mentioned above, in this limit the two-dimensional return map collapses to a one-dimensional circle map. In theory this is straightforward. In practice, however, considerable care must be exercised in many cases, such as the model of Ref. 6. The reason is that the location of the limit cycle in general depends on that parameter which is a measure of the inverse relaxation time for perturbations off the limit cycle, and, consequently, the model may not have a definite limit cycle in the fast-relaxation limit. As a result, the differential equations cannot be reduced to a one-dimensional map without variable scaling. The model of the present paper, however, is such that the location of limit cycle is independent of the relaxation parameter, and consequently an exact one-dimensional return map will be obtained without difficulties.

Notice that the resulting one-dimensional map has topologically different properties for strong and weak external force, and is nonanalytic for a critical strength of the external force. This nonanalyticity is not a mathematical abstraction, but owes its existence to the unstable fixed point inside the limit cycle, thus generic in nature. Two examples are shown in Figs. 1(a) and 1(b). The Brusselator[3,4] describes a hypothetical three-molecular chemical reaction with an autocatalytic step under far from equilibrium conditions. The external force is here assumed to consist of rectangular pulses [Fig. 1(a)]. Figure 1(b)

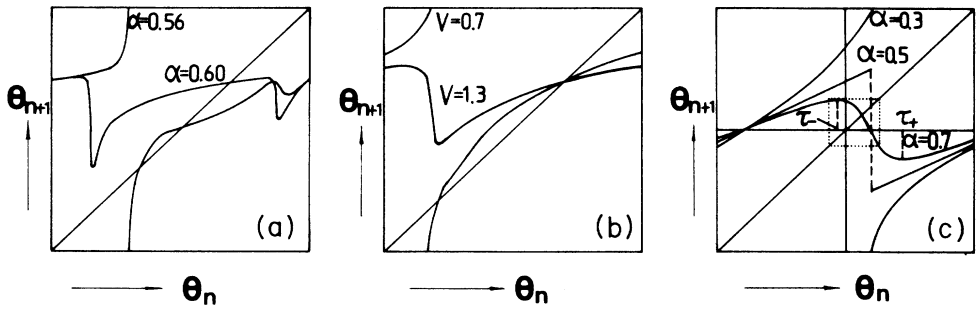

FIG. 1. Circle maps $\theta_{n+1}=f(\theta_n)$ for three models. (a) The forced Brusselator $\dot{x}=2-9x+x^2y+F$, $\dot{y}=8x-x^2y$, $F=\alpha$ if $10n<t<10n+5$, or $F=0$ if $10n+5<t<10(n+1)$, with integer n. The critical strength here is $\alpha_c\doteq 0.58$. (b) An electronic oscillator (see Ref. 6) $\ddot{x}+\pi(20x^2-1)\dot{x}+0.5\pi^2x(50x^4-10x^2+1)=V\sum_n\delta(t-4n)$. The critical strength here is $V_c\doteq 1.0$. (c) Three topologically different versions of the prototype map (2.7) with $\beta=0.4$.

represents an electronic oscillator tuned with nonlinear elements and having its frequency synchronized by means of an external impulsive periodic signal.[6] In each example the circle map exhibits topologically different properties for force amplitudes bigger or less a critical strength. Thus a nonanalyticity must take place when the external force has a critical strength. Because of the difficulty mentioned above, these two examples are not really limiting cases, though the relaxation time is very short. One may presume that a set of rescaled variables will make the limit cycle definite in the fast relaxation limit.

The motivation of the present paper is to reveal the structure of parameter space for a wide class of nonlinear driven oscillators. This class is characterized as follows. (i) The free nonlinear oscillator has a stable limit cycle, which encloses an unstable stationary point. (ii) The external force is such that above and below a critical strength the circle map exhibits topologically different properties. It is clear that the present circle map is qualitatively different from the sine map which has been investigated in great detail.[10,11] A brief account of some results of the present study have already been published.[12]

The remaining part of the article is organized as follows. In Sec. II a prototype model of nonlinear driven oscillators is introduced, and transformed into a one-dimensional circle map in the fast relaxation limit. The weak force and the borderline situations are treated in Sec. III, while the more interesting and more complex strong-force situation is discussed in the successive sections.

II. THE MODEL

The shape and the location of the limit cycle may be changed by a transformation of variables, and as a prototype two-dimensional nonlinear oscillator with a stable limit cycle we can take

$$\dot{r}=sr(1-r^2)\ ,\quad \dot{\theta}=1 \tag{2.1}$$

in a properly scaled polar coordinate. The parameter s is a measure of the inverse relaxation time for perturbations off the limit cycle $r=1$. This oscillator is subjected to a periodic force in the x direction, with the following evolution equations

$$\begin{aligned}\dot{x}&=sx(1-x^2-y^2)-y+2\alpha\sum_n\delta(t-2\pi n\beta)\ ,\\ \dot{y}&=x+sy(1-x^2-y^2)\ ,\end{aligned} \tag{2.2}$$

with $\beta>0$. The summation is over all integers n, and

$$x=r\cos\theta\ ,\quad y=r\sin\theta\ . \tag{2.3}$$

We now make a "stroboscopic" map of the dynamics, focusing on the values x_n, y_n, r_n, and θ_n of x, y, r, and θ immediately after the nth "kick" at time $t=2\pi n\beta$. We denote the values of these variables immediately before the $(n+1)$th "kick" at time $t=2\pi(n+1)\beta$ by x_n^*, y_n^*, r_n^*, and θ_n^*. It is quite easy to deduce from Eqs. (2.1) that

$$r_n^*=\frac{r_n}{[r_n^2+(1-r_n^2)e^{-4\pi\gamma}]^{1/2}}\ ,\quad \theta_n^*=\theta_n+2\pi\beta \tag{2.4}$$

with $\gamma=s\beta$, since no external force acts on the oscillator between two successive "kicks." Furthermore, integrating both sides of the Equations (2.2) from time $t=2\pi(n+1)\beta-\epsilon$ to $t=2\pi(n+1)\beta+\epsilon$, we find in the limit $\epsilon\to 0$ that

$$\begin{aligned}x_{n+1}&=x_n^*+2\alpha=r_n^*\cos\theta_n^*+2\alpha\ ,\\ y_{n+1}&=y_n^*=r_n^*\sin\theta_n^*\ .\end{aligned} \tag{2.5}$$

Thus we obtain the following two-dimensional return map

$$\begin{aligned}r_{n+1}&=\{[2\alpha+r_n^*\cos(\theta_n+2\pi\beta)]^2\\ &\quad+[r_n^*\sin(\theta_n+2\pi\beta)]^2\}^{1/2}\ ,\\ \tan\theta_{n+1}&=\frac{r_n^*\sin(\theta_n+2\pi\beta)}{2\alpha+r_n^*\cos(\theta_n+2\pi\beta)}\ ,\end{aligned} \tag{2.6}$$

with r_n^* defined by (2.4). The uniqueness of the iteration is guaranteed by the implicit requirements that y_{n+1} and $\sin(\theta_n+2\pi\beta)$ have the same sign, i.e., $\sin\theta_{n+1}$ and $\sin(\theta_n+2\pi\beta)$ have the same sign. When $r_{n+1}=0$, the value of θ_{n+1} is arbitrary. However, the next iteration gives a unique θ_{n+1} as long as $\alpha\neq 0$.

Taking $\gamma\to\infty$, the fast-relaxation limit, we obtain from Eq. (2.4) that $r_n^*=1$. This reflects the obvious result that the oscillator returns to its limit cycle before the next "kick." In this limit we get from Eqs. (2.6) that the posi-

tion on the circle satisfies

$$\theta_{n+1}=f(\theta_n)\ ,\quad \tan\theta_{n+1}=\frac{\sin(\theta_n+2\pi\beta)}{2\alpha+\cos(\theta_n+2\pi\beta)} \tag{2.7}$$

a one-dimensional circle map with two parameters. Here α is the measure of the amplitude of the external force and β is the ratio of two frequencies. Without loss of generality we may assume $\alpha\geq 0$, $0<\beta\leq 1$, and $-\pi<\theta_n\leq\pi$. The iteration, shown in Fig. 1(c), has completely different properties in the three cases $\alpha<\frac{1}{2}$, $\alpha=\frac{1}{2}$, and $\alpha>\frac{1}{2}$. The map is invertible for $\alpha<\frac{1}{2}$ (weak force), piecewise linear for $\alpha=\frac{1}{2}$ (the borderline case), and noninvertible for $\alpha>\frac{1}{2}$ (strong force). As mentioned in the Introduction, the nonanalyticity of map (2.7) is by no means unphysical. It is universal for a wide class of driven oscillators, since this nonanalyticity corresponds to a force just sufficiently strong to displace the oscillator into the unstable stationary point (the origin in the present model). Note also that since the mapping (2.7) is symmetric (with $\theta\rightarrow-\theta$) about $\beta=\frac{1}{2}$ it suffices to discuss $\beta\leq\frac{1}{2}$.

The numerical results, of which a few are shown in Fig. 2(a), display the complicated structure of the parameter

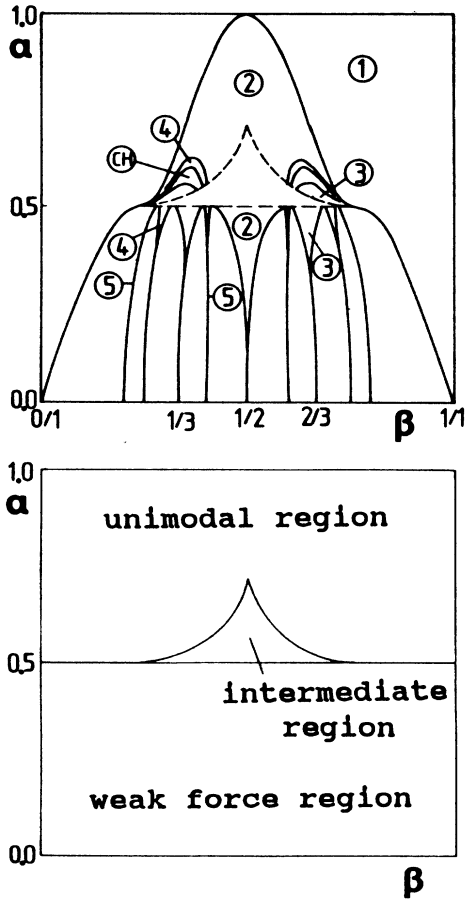

FIG. 2. (a) Location of some periodic (the numbers inside circles indicate the length) and chaotic regions for the map (2.7). (b) The three regions in the parameter space. In the intermediate region the state of the system may depend on the initial condition.

space. We can divide the parameter space into the following three regions [see Fig. 2(b)].

(i) In the weak-force region $\alpha\leq\frac{1}{2}$, the system displays mode-locking and quasiperiodic behavior. Mode locking for each (rational) winding number[8] P/Q takes place in an interval of β. In case $\alpha\rightarrow 0$, the width of every mode-locking interval tends to zero, so the probability that the winding number is rational, for a random value of β, will tend to zero. With increasing value of α the width of mode-locking intervals (so-called "Arnol'd tongues") increase.

(ii) In the unimodal region $\alpha>\alpha_t$, where

$$\alpha_t=\begin{cases}\dfrac{1}{2\sin[(\frac{3}{4}-\beta)\pi]} & \text{for } \frac{1}{4}\leq\beta\leq\frac{1}{2}\ ,\\ \dfrac{1}{2\sin[(\beta-\frac{1}{4})\pi]} & \text{for } \frac{1}{2}<\beta\leq\frac{3}{4}\ ,\\ \frac{1}{2} & \text{otherwise}\ ,\end{cases} \tag{2.8}$$

period-doubling bifurcation and chaotic behavior are found. The order of the period orbits is arranged according to the Metropolis-Stein-Stein U ("Universal") sequences.[13] The formula (2.8) will be explained in Sec. IV. The word "unimodal" here means that the mapping has only one extremum. The stable orbit for a unimodal mapping is independent of the initial condition.[8]

(iii) In the intermediate region $\frac{1}{4}\leq\beta\leq\frac{3}{4}$ and $\frac{1}{2}<\alpha\leq\alpha_t$ the transition between the unimodal mapping and the mode locking behavior takes place, and many new sequences of periodic orbits occur.

Both regions (ii) and (iii) represent the strong-force situation. We will discuss these regions one by one in the successive sections.

It should be emphasized here that numerical investigations for the two-dimensional map (2.6) with $\gamma=1$ gives almost the same results as the limiting case.[9] The one-dimensional mapping is, therefore, *representative* for the more general finite-relaxation-time situation.

III. THE WEAK-FORCE REGION, $\alpha\leq\frac{1}{2}$

For $\alpha\leq\frac{1}{2}$ the mapping function (2.7) has a discontinuous point, and is divided into two continuous branches by this point, as shown in Fig. 1(c). The discontinuosity for case $\alpha<\frac{1}{2}$ comes from the restriction that the mapping is modulated by 2π, and it can be removed when the right branch is lifted by 2π. If an orbit constructed of Q's iterations visits the right branch of the mapping by P times, we call the ration $w=P/Q$ for *winding number*. It is obvious that this definition for the winding number is the same as usual one.[8,10]

The dynamics for case $\alpha<\frac{1}{2}$ is simple. The mapping (2.7) is invertible, since it has positive slope everywhere:

$$\frac{d\theta_{n+1}}{d\theta_n}=\frac{1+2\alpha\cos(\theta_n+2\pi\beta)}{1+4\alpha\cos(\theta_n+2\pi\beta)+4\alpha^2}>0\quad\text{for } \alpha<\frac{1}{2}\ . \tag{3.1}$$

Then we know that system displays quasiperiodic or

periodic behavior in this region.[8] The properties of the mapping (2.7) for $\alpha<\frac{1}{2}$ are quite similar to that of the subcritical sine circle map.[10,11] In fact, we may expand (2.7) for small α, and get

$$\theta_{n+1}=\theta_n+2\pi\beta+2\alpha\sin(\theta_n+2\pi\beta)+O(\alpha^2) \pmod{2\pi}, \tag{3.2}$$

which is nothing but the sine circle map.

It is easy to see that mode locking with winding number $w=0/1$ or $w=1/1$ (fixed points) occurs when $\beta=0$ or $\beta=1$, since the mapping (2.7) intersects the line $\theta_{n+1}=\theta_n$. The limiting situation for this mode-locking case is that the mapping (2.7) is tangential to the diagonal $\theta_{n+1}=\theta_n$. Thus the boundary for the $w=0/1$ and $w=1/1$ mode-locking regions in parameter space are determined by the equations

$$\frac{d\theta_{n+1}}{d\theta_n}=1, \qquad \theta_{n+1}=\theta_n, \tag{3.3}$$

which have solutions

$$\alpha=\tfrac{1}{2}\sin(2\pi\beta) \quad \text{for } \beta<\tfrac{1}{2} \tag{3.4}$$

and

$$\alpha=-\tfrac{1}{2}\sin(2\pi\beta) \quad \text{for } \beta>\tfrac{1}{2}. \tag{3.5}$$

The widths of both these mode-locking intervals of β increase when α increases. The boundaries for other mode-locking regions can be calculated similarly, and the results are shown in Fig. 3. All the "Arnol'd tongues" increase their widths as α increases. However, they never overlap in the weak-force region.

At the borderline $\alpha=\frac{1}{2}$ I use $[P/Q]$ to denote the region of β where mode locking with winding number P/Q takes place. An exact calculation[14] shows that the complimentary set of the mode-locking intervals is a Cantor set with dimension $D=0$. This conclusion is correct for the class of piecewise linear mappings with any constant slope less than 1 in magnitude.[14]

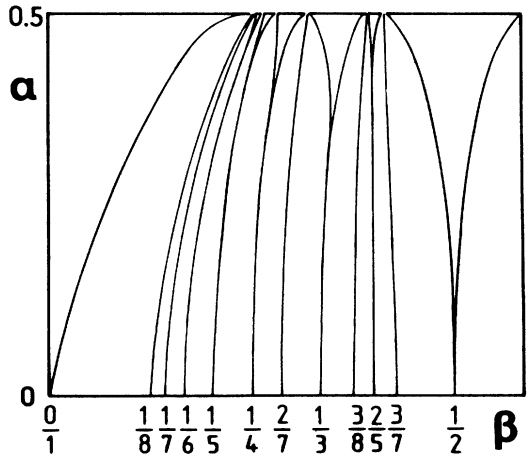

FIG. 3. The mode-locking regions in the weak-force region.

For $\alpha=\frac{1}{2}$ the mapping is discontinuous at the point

$$\tau=(1-2\beta)\pi. \tag{3.6}$$

The left branch is called L, and the right one R. Thus each orbit can be characterized by a "word" constructed of R's and L's, according to whether the iteration is on the right or the left branch. Periodic orbits that visit the right end point of the branch L, or the left end point of the branch R, we call *superstable orbits.* Taking the end point as the initial point the corresponding words start with the letter L or R, respectively. The word W for the left end point of $[P/Q]$ may be determined by means of the following theorem (theorem 1). Let

$$w=\frac{P}{Q}=\cfrac{1}{N_1+\cfrac{1}{N_2+\cfrac{1}{\cdots+\cfrac{1}{N_j}}}} \tag{3.7}$$

be the simple continued-fraction representation of w with positive integers $N_1,N_2,\ldots,N_j$. Then the words W_j corresponding to the left end points of the mode-locking regions $[P/Q]$ can be constructed by the following recursive prescription:

$$\begin{aligned} &W_1=RL^{N_1-1}, \\ &W_2=W_1LW_1^{N_2-1}, \\ &W_j=W_{j-1}^{N_j}W_{j-2} \quad \text{for odd } j\geq 3, \\ &W_j=W_{j-2}W_{j-1}^{N_j} \quad \text{for even } j\geq 4. \end{aligned} \tag{3.8}$$

The proof of this theorem is relegated to the Appendix.

The word $\hat{W}$ for the right end point of the mode-locking region $[P/Q]$ can be obtained from the word W for the left end point of the same region $[P/Q]$ by interchanging the first two letters, R and L. In other words, if

$$W=RLX, \tag{3.9}$$

then we have

$$\hat{W}=LRX, \tag{3.10}$$

where X is a syllabus of R's and L's.[14]

The value β of an end point corresponding to a word W can be calculated by the formula[14]

$$\beta=\frac{W1-1}{4(2^Q-1)}. \tag{3.11}$$

Here W is an operator operating on numbers, and identical in form with the word of the end point, thus composed of operators R and L, defined through

$$Lx=2x, \quad Rx=2(x+1). \tag{3.12}$$

The mode-locking regions and the corresponding symbolic dynamics words for the interval end points at $\alpha=\frac{1}{2}$ with $w\leq\frac{1}{2}$ and $Q\leq 8$ are listed in Table I. Corresponding results for $\frac{1}{2}<w\leq 1$ may be obtained by using the symmetry of the mapping about $\beta=\frac{1}{2}$. The intervals for the

TABLE I. The mode-locking regions (period ≤ 8 only) at $\alpha=\frac{1}{2}$ with $P/Q \leq \frac{1}{2}$.

Order	$[P/Q]$	Words	β interval
1	[0/1]	$-, L$	[0,0.25000]
2	[1/8]	RL^7, LRL^6	[0.25196,0.25392]
3	[1/7]	RL^6, LRL^5	[0.25394,0.25787]
4	[1/6]	RL^5, LRL^4	[0.25794,0.26587]
5	[1/5]	RL^4, LRL^3	[0.26613,0.28226]
6	[1/4]	RL^3, LRL^2	[0.28334,0.31667]
7	[2/7]	RL^3RL^2, LRL^2RL^2	[0.31693,0.32087]
8	[1/3]	RL^2, LRL	[0.32143,0.39286]
9	[3/8]	$RL^2RL^2RL, LRLRL^2RL$	[0.39314,0.39510]
10	[2/5]	$RL^2RL, LRLRL$	[0.39516,0.41129]
11	[3/7]	$RL^2RLRL, LRLRLRL$	[0.41142,0.41535]
12	[1/2]	RL, LR	[0.41667,0.58333]

winding numbers w and $1-w$ are symmetrically placed on each side of $\beta=\frac{1}{2}$. The word at $\beta=1-\beta'$ is the same as at $\beta=\beta'$, except that all R's are turned into L's and vice versa. For example, for the right end point of [2/3] we obtain the word $W=LR^2$ which is just the "symmetric word" to RL^2, the word for the left end point of [1/3] at $\beta=\frac{9}{28}$, and the corresponding value of β is $1-\frac{9}{28}=\frac{19}{28}$.

If we keep $\alpha=\frac{1}{2}$ and let the value of β increase from 0 to 1, we will find a series of periodic orbits. Each periodic orbit in this series corresponds to a rational winding number w, and its period is the demonimator of this fraction. The ordering is simply according to the magnitude of w. For periods not exceeding a given integer N the winding numbers are the ordered set of all positive rationals less than unity, in number theory[15] called the Farey series of order N. The infinite ordered collection of all periodic orbits we call the *Farey sequence.*

IV. THE UNIMODAL REGION

Now we are in a position to discuss the more complicated region $\alpha > \frac{1}{2}$. In fact, it suffices to consider the region $\frac{1}{2} < \alpha < 1$, since $\alpha \geq 1$ corresponds to the very strong external force situation where $|f'(\theta)| \leq 1$ and the stable orbit of the system has period 1.

For $\alpha > \frac{1}{2}$ the mapping function $f(\theta)$, Eq. (2.7), has a maximum

$$\theta_m = f(\tau_-) \tag{4.1}$$

and a minimum

$$-\theta_m = f(\tau_+) , \tag{4.2}$$

where

$$\tau_\pm = (1-2\beta)\pi \pm \cos^{-1}(1/2\alpha) \tag{4.3}$$

and

$$\theta_m = \sin^{-1}(1/2\alpha) . \tag{4.4}$$

A period orbit visiting the maximum or the minimum is called a *superstable orbit.* We will discuss two types: class-1 orbits start from the maximum at τ_-, while class-2 orbits start from the minimum at τ_+. The superstable orbits previously introduced for $\alpha=\frac{1}{2}$ are clearly special cases.

Each periodic orbit corresponds to a finite word constructed of L's, M's, and R's. For superstable orbits the first letter, L or R, denotes whether the orbit starts from the maximum at τ_- or from the minimum at τ_+, and the subsequent letters L, M, or R denote whether the successive iterations fall in the interval $(-\pi,\tau_-]$, (τ_-,τ_+), or $[\tau_+,\pi]$, respectively. That is to say, we have the designation

$$\begin{aligned} &L \text{ if } \theta \leq \tau_- , \\ &M \text{ if } \tau_- < \theta < \tau_+ , \\ &R \text{ if } \theta \geq \tau_+ , \end{aligned} \tag{4.5}$$

for the letters in the word of the superstable orbit. Thus the superstable orbits of class 1 have words starting with the letter L, while those of class 2 have words starting with R. The word corresponding to a period-N orbit consists of N letters altogether. Notice that our definition of words is in close agreement with that used by Metropolis *et al.*[13] for the simpler case of unimodal mappings. In the present case the unimodal mapping takes place using the branches L and M, so for this case our notation differs from the standard symbolic-dynamics notation[13] in two ways: R must be replaced by M, and, in addition, an L for the starting point must be added (omitted in the standard Metropolis-Stein-Stein notation).

Let us denote the line in our parameter space (α,β) for which a given superstable orbit exists, as a *trajectory.* We will use the same symbolic dynamics word to denote both a superstable orbit and the corresponding trajectory. Thus trajectories are divided into two classes, according to whether the orbits belong to class 1 or class 2. All trajectories must start and end at the endpoints of the periodic intervals $[P/Q]$ as α tends to $\frac{1}{2}$, since both τ_- and τ_+ tend to τ in this limiting case. Figure 4 illustrates this notion.

Another class of orbits, called *pseudo-orbits* will be useful for the discussion. A pseudo-orbit of class 1 or 2 is defined as a nonperiodic orbit that starts from the maximum at $\theta=\tau_-$ and ends at the minimum at $\theta=\tau_+$, or

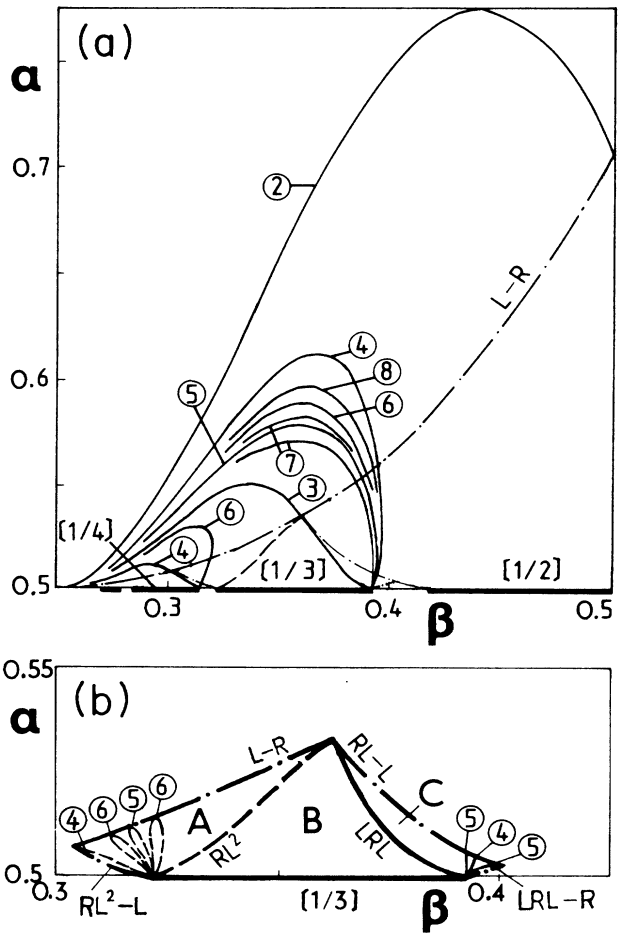

FIG. 4. (a) Some trajectories of class 1 for superstable orbits of U sequence (solid lines). Numbers inside circles indicate the period. Dotted-dashed lines indicate pseudotrajectories. (b) The pentagon connected to the interval [1/3]. The dashed lines are trajectories of class 2 which do not belong to the U sequence (see Sec. VI).

starts from the minimum and ends at the maximum, respectively. Notice that $(N+1)$ letters are needed to denote the pseudo-orbit made of N iterations, since the last letter is used to identify its end point. We put a dash before the last letter in the word for a pseudo-orbit to distinguish it for that of superstable orbit. For example, the pseudo-orbit starting from $\theta=\tau_-$ and reaching $\theta=\tau_+$ by one iteration, i.e., $\tau_+=f(\tau_-)$, has the word $R-L$. The length of the word, the number of iterations, is 1 in this case. The line in parameter space for which a given pseudo-orbit exists is called a *pseudotrajectory*. We will use the same symbolic dynamics word to denote both the pseudo-orbit and the corresponding pseudotrajectory.

Let us consider the pseudotrajectory $L-R$, which is determined by the equation $\tau_+=f(\tau_-)$, i.e.,

$$\theta_m=\tau_+$$

by the definition (4.1). Using (4.3) and (4.4) we get

$$\sin^{-1}(1/2\alpha)=(1-2\beta)\pi+\cos^{-1}(1/2\alpha)$$

with solution

$$\alpha=\frac{1}{2\sin[(\frac{3}{4}-\beta)\pi]} \quad \text{for } \tfrac{1}{4}\le\beta<\tfrac{3}{4} . \tag{4.6}$$

Similarly the pseudotrajectory $R-L$ is determined by the equation

$$\alpha=\frac{1}{2\sin[(\beta-\frac{1}{4})\pi]} \quad \text{for } \tfrac{1}{4}<\beta\le\tfrac{3}{4} . \tag{4.7}$$

These two pseudotrajectories $R-L$ and $L-R$ will be very important in our discussion of the structure of the parameter space. The Eqs. (4.6) and (4.7) agree for $\frac{1}{4}\le\beta\le\frac{3}{4}$ with the definition (2.8) of α_t, the lower boundary of the unimodal region in parameter space. When $\alpha\ge\alpha_t$, the iterates are confined to a region where $f(\theta)$ is unimodal [the dotted square in Fig. 1(c)], and all the usual[8,13,16] period-doubling bifurcation sequences, chaotic behavior, etc., are found. In particular, the order of appearance of the stable orbits is given by the universal sequence, the U sequence.[13] As we have mentioned, however, the words we use here are somewhat different from the standard words, which are constructed of R's and L's, according to whether successive iterations of the maximum falls to the right or the left of the maximum. To have the ordering given by the universal sequence one must follow directions in parameter space that intersects each trajectory once (see Fig. 4), along $\alpha=\alpha_t(\beta)$, for instance. Results for this choice are shown for periods not longer than 8 in Table II. Since these superstable orbits visit both the maximum and the minimum, the Feigenbaum convergence rate for period-doubling bifurcations is $\delta=7.284\ldots$, representative for the universality class[17] $x_{n+1}=f(x_n)=1-\mu x_n^4+\cdots$. The results for the series of bifurcations are shown in Table III.

V. THE INTERMEDIATE REGION

The region $\frac{1}{2}<\alpha\le\alpha_t$, $\frac{1}{4}\le\beta\le\frac{3}{4}$ is the most complicated part of the parameter space [Fig. 2(b)]. This region must contain an interpolation between the U-sequence systematics along $\alpha=\alpha_t$ and the mode-locking behavior at $\alpha=\frac{1}{2}$. Furthermore, as we will show later, there are many new sequences of periodic orbits in this region of parameter space. In this section we will study the general systematics of periodic orbits. Several new sequences of periodic orbits will be given in Sec. VI.

Consider S_2, the point of intersection between the pseudotrajectories $R-L$ and $L-R$. It is known from the solutions of the Eqs. (4.6) and (4.7) that this point is $\beta=\frac{1}{2}$ and $\alpha=\sqrt{2}/2$. It is evident that the trajectories RL and LR must both pass through this point. The trajectory RL is determined by the equation $\tau_+=f^{(2)}(\tau_+)$, i.e., $\tau_+=f(-\theta_m)$ by Eq. (4.2). On the other hand, we may obtain from the map (2.7) that $\sin(\theta_n-\theta_{n+1}+2\pi\beta)=2\alpha\sin\theta_{n+1}$. Thus $\tau_+=f(-\theta_m)$ means $\sin(-\theta_m-\tau_++2\pi\beta)=2\alpha\sin\tau_+$, i.e.,

$$\cos(4\pi\beta)=2\alpha\sin[2\pi\beta-\cos^{-1}(1/2\alpha)] . \tag{5.1}$$

TABLE II. The U sequence along the pseudotrajectory $L-R$.

Order	Period[a]	β[b]	Word
1	2	0.500 000 000 000	LR
2	4	0.394 627 357 428	$LRLM$
3	8	0.390 658 086 411	$LRLM^3LM$
4	6	0.389 533 259 406	$LRLM^3$
5	8	0.389 391 022 362	$LRLM^5$
6	7	0.389 361 753 097	$LRLM^4$
7	5	0.388 543 703 305	$LRLM^2$
8	7	0.384 566 789 160	$LRLM^2LM$
9	8	0.383 278 376 272	$LRLM^2LM^2$
10	3	0.362 430 412 114	LRL
11	6	0.319 517 205 258	LRL^2ML
12	8	0.318 664 122 804	LRL^2MLM^2
13	7	0.318 569 709 261	LRL^2MLM
14	8	0.318 379 894 662	LRL^2MLML
15	5	0.316 213 841 961	LRL^2M
16	8	0.314 948 079 153	LRL^2M^3L
17	7	0.314 895 679 561	LRL^2M^3
18	8	0.314 870 893 681	LRL^2M^4
19	6	0.314 701 624 103	LRL^2M^2
20	8	0.314 401 958 143	LRL^2M^2LM
21	7	0.314 293 824 499	LRL^2M^2L
22	4	0.303 583 635 838	LRL^2
23	8	0.283 741 748 726	LRL^3ML^2
24	7	0.283 105 404 837	LRL^3ML
25	8	0.282 896 168 745	LRL^3MLM
26	6	0.282 034 031 851	LRL^3M
27	8	0.281 470 411 553	LRL^3M^3
28	7	0.281 392 493 400	LRL^3M^2
29	8	0.281 258 732 144	LRL^3M^2L
30	5	0.276 170 302 316	LRL^3
31	8	0.266 257 577 043	LRL^4ML
32	7	0.265 773 128 482	LRL^4M
33	8	0.265 468 785 932	LRL^4M^2
34	6	0.262 930 313 250	LRL^4
35	8	0.257 827 074 717	LRL^5M
36	7	0.256 425 985 315	LRL^5
37	8	0.253 203 072 843	LRL^6

[a]Period ≤ 8 only.
[b]For superstable orbit.

Similarly, the trajectory LR is determined by the equation

$$-\cos(4\pi\beta)=2\alpha\sin[2\pi\beta+\cos^{-1}(1/2\alpha)]\ , \tag{5.2}$$

and the pseudotrajectories $RL-L$ and $LR-R$ by the equations

$$\cos[4\pi\beta+2\cos^{-1}(1/2\alpha)] =2\alpha\sin[(1-2\beta)\pi-\cos^{-1}(1/2\alpha)] \tag{5.3}$$

and

$$-\cos[4\pi\beta-2\cos^{-1}(1/2\alpha)] =2\alpha\sin[(1-2\beta)\pi+\cos^{-1}(1/2\alpha)]\ , \tag{5.4}$$

respectively. The pseudotrajectories $L-R$, $RL-L$, $LR-R$, $R-L$, and the trajectories LR and RL are shown in Fig. 5. These four pseudotrajectories and the interval

TABLE III. A sequence of period-doubling bifurcations along the pseudotrajectory $L-R$. The β values for the superstable orbits and the corresponding Feigenbaum convergence rate δ (calculated as a ratio of two successive β intervals) are shown.

Order	Period	β	δ
1	2	0.500 000 000 000 00	
2	4	0.394 627 357 427 62	
3	8	0.390 658 086 411 00	26.5471
4	16	0.390 322 422 047 25	11.8251
5	32	0.390 279 322 753 92	7.7882
6	64	0.390 273 566 515 65	7.4874
7	128	0.390 272 781 971 93	7.3371
8	256	0.390 272 674 516 12	7.3011
9	512	0.390 272 659 774 76	7.2894
10	1024	0.390 272 657 751 53	7.2861
11	2048	0.390 272 657 473 81	7.2851
12	4096	0.390 272 657 435 69	7.2848
13	8192	0.390 272 657 430 45	7.2842

[1/2] at $\alpha=\frac{1}{2}$ form a pentagon-shaped domain in the parameter space (for brevity called a "pentagon" from now on). The trajectories RL and LR divide the pentagon into three triangular areas, A, B, and C, see Fig. 5. Area A has three sides represented by the words $L-R$, $RL-L$, and RL. Let us denote the part of a word before the first letter M as the prefix. Then it follows that all trajectories of class 2 in this triangular area have words with prefix RL, since they are between the two lines $RL-L$ (third iteration at τ_+) and RL (third iteration at τ_-), and the third iteration must by continuity fall on (τ_-,τ_+). In the limit $\alpha\to\frac{1}{2}^+$ the middle part (M) of the mapping $f(\theta)$ becomes vertical, and all these orbits with prefix RL now become in this limit periodic with period 2 and with word $W=RL$. Since the orbits visit the discontinuity point of the piecewise linear $\alpha=\frac{1}{2}$ map, the corresponding value of β will represent the left end point of the periodic interval [1/2].

By similar considerations as above, it is easy to show that all the trajectories of class 1 in the triangular domain C have words with prefix LR. They terminate for $\alpha\to\frac{1}{2}^+$ at the right endpoint of [1/2], since they are located between the lines LR and $LR-R$.

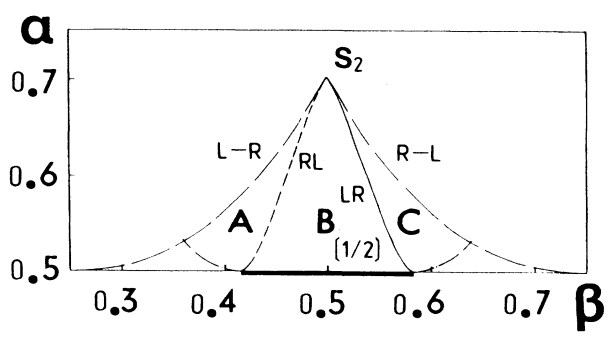

FIG. 5. Pentagon connected to the interval [1/2].

For values of α and β in the triangular domain B, the system has a stable period-2 orbit, independent of the initial value. In order to prove this result, let us consider the function $G_2(\theta,\beta)=f(f(\theta))-\theta$ for a fixed $\alpha=\alpha_a>\frac{1}{2}$, and let β increase from β_2, corresponding to the trajectory RL, to β_3, corresponding to the trajectory LR. It is evident that $G_2(\tau_+,\beta_2)=f(-\theta_m)-\tau_+=0$, corresponding to a superstable orbit of class 2. As β increases from β_2, $G_2(\tau_+,\beta)$ will be positive, since $f(-\theta_m)$ increases and τ_+ decreases, by Eqs. (2.7) and (4.3). However, $G_2(\pi,\beta)$ is never positive. Thus we find that $G_2(\theta,\beta)=0$ has at least one root in the interval (τ_+,π) for $\beta_2<\beta$. Similarly, we can find that $G_2(\theta,\beta)=0$ has at least one root in region $(-\pi,\tau_-)$ for $\beta<\beta_3$. So an orbit with period 2 is always present for any (α,β) with $\beta_2<\beta<\beta_3$. It remains to prove stability. The period-2 orbit visits the right branch R or the left branch L, or both, but we can show that it never visits the middle branch M. To prove this let us define ξ_- on branch L such that $f(\xi_-)=\tau_+$, and ξ_+ on branch R such that $f(\xi_+)=\tau_-$, see Fig. 6. Since $G_2(\tau_+,\beta)$ is positive, we know that $f(-\theta_m)>\tau_+$, thus $\xi_-<-\theta_m$. Similarly, we have $\xi_+>\theta_m$. Assume, hypothetically, that the orbit visits the middle branch M at the nth iterate, i.e., $\tau_-<\theta_n<\tau_+$. Then the last iterate θ_{n-1} must also fall on branch M. [Otherwise, $\theta_{n-1}>\xi_+$ or $\theta_{n-1}<\xi_-$, which is impossible since $|f(\theta)|\le\theta_m$.] Hence the orbit has to be confined to the middle branch M from the beginning, which is not true. The conclusion is, therefore, that the period-2 orbit mentioned above will never visit the middle branch M. Since $|f'(\theta)|<1$ for the two branches R and L it actually visits, the orbit of period 2 must be stable.

Above we have found analytic expressions for several simplest trajectories and pseudotrajectories. In principle, this method may be used to find analytic expressions for trajectories of orbits with longer periods. However, that would be rather time consuming. It is in most cases more efficient to use numerical methods to find trajectories or pseudotrajectories in parameter space. The question is how this infinite collection of trajectories can be given structure and order. We will now explain how the parameter space can be subdivided into regions with a hierarchal structure. This hierarchal ordering is connected with trajectory systematics.

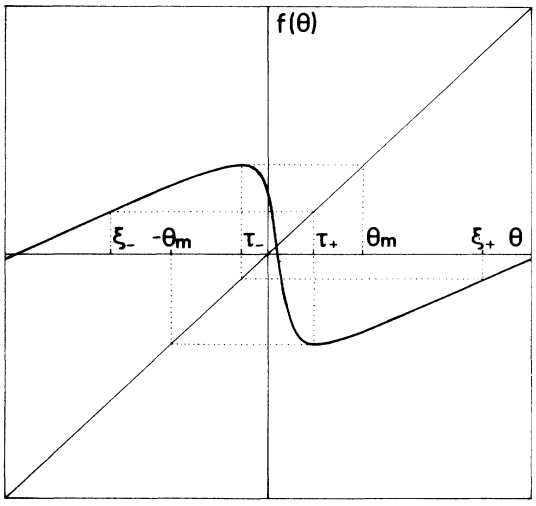

FIG. 6. The mapping (2.7) for $\alpha=0.55$ and $\beta=0.48$, parameter values within the area B in Fig. 5.

Let us consider at the critical line $\alpha=\frac{1}{2}$ the set of all mode-locking regions whose inverse winding numbers are integers, i.e.,

$$\ldots,[1/N_1],[1/(N_1-1)],\ldots,[1/4],[1/3],[1/2]\ . \quad (5.5)$$

Let

$$F_n(\beta)\equiv f^{(n)}(\tau_+)-\tau_-\ ,$$

where the value of α is taken to be $\alpha_t(\beta)$. At S_2, the point of intersection between the pseudotrajectory $L-R$ and $R-L$ we have $F_2(\beta)=\tau_+-\tau_->0$. At S, the right end point of the interval [0/1], however, we have $F_2(\beta)<0$. Thus we know that $F_2(\beta)=0$ must have a root between S and S_2. So we can find a point on the pseudotrajectory $L-R$, say S_3, which must be visited by the pseudotrajectory $RL-L$. Moreover, at point S_3 we have $F_3(\beta)=\tau_+-\tau_->0$. At point S we still have $F_3(\beta)<0$. Thus we know that a point S_4 between S and S_3 on the pseudotrajectory $L-R$ must be visited by the pseudotrajectory RL^2-L. We may go in this way and find a series of points along the pseudotrajectory $L-R$, say S_{N_1} with $N_1=3,4,\ldots$, which must be visited by the pseudotrajectories $RL^{N_1-2}-L$ with $N_1=3,4,\ldots$, respectively. Notice that the pseudotrajectory RL^{N_1-2} must end at the left end point of the interval $[1/(N_1-1)]$ when $\alpha\to\frac{1}{2}$ from above, and that the series of points S_{N_1} and the series of intervals $[1/(N_1-1)]$ have the same relative ordering [see Fig. 7(a)]. We can similarly show that a series of pseudotrajectories $LRL^{N_1-2}-R$ must be present, and that each of them connects the right end point of $[1/N_1]$ to a point on the pseudotrajectory $RL^{N_1-2}-L$ between S_{N_1} and the left end point of $[1/(N_1-1)]$. Hence above any interval in (5.5), say $[1/N_1]$, we have a similar pentagon-shaped domain as described above for [1/2]. The left end point of $[1/N_1]$ is associated with a word $W_1=RL^{N_1-1}$ and its right end point with a word $\hat{W}_1=LRL^{N_1-2}$. A pseudotrajectory with word $RL^{N_1-1}-L$ starts at the left end point of $[1/N_1]$, and a pseudotrajectory with word $LRL^{N_1-2}-R$ starts at the right end point of $[1/N_1]$. There are two such pseudotrajectories for each mode-locking region in (5.5), and a series of pentagons, shown in Fig. 7(a), can now be constructed. The pentagon immediately above $[1/N_1]$ is enclosed by parts of the pseudotrajectories $L-R$, $RL^{N_1-2}-L$, $LRL^{N_1-2}-R$, $RL^{N_1-1}-L$, and by $[1/N_1]$ itself.

The point of intersection between $L-R$ and $RL^{N_1-2}-L$ must be visited by the trajectory of class 1 with word LRL^{N_1-2} and that of class 2 with word RL^{N_1-1}. These two trajectories divide the pentagon above $[1/N_1]$ into three triangular areas A, B, and C, shown in Fig. 7(b).

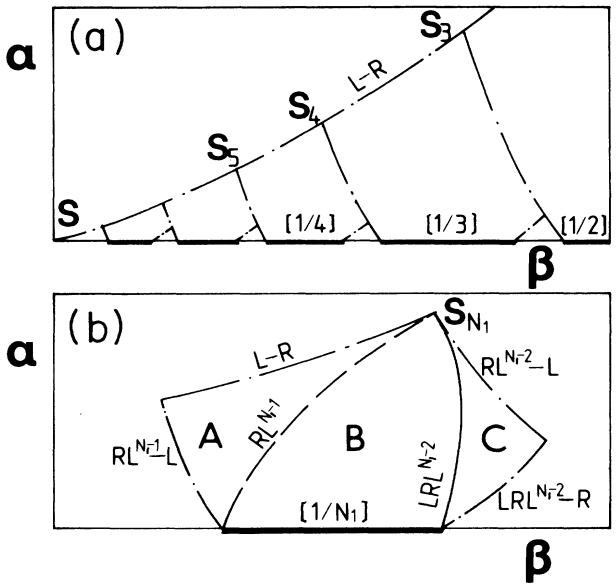

FIG. 7. (a) Pentagons connected to intervals of the first level (sketched only). (b) Blowup of the pentagon immediately above the interval $[1/N_1]$.

It is easy to see that all the trajectories of class 2 in the area A have words with prefix RL^{N_1-1}. In fact, denote the N_1th iteration of $\theta_1=\tau_+$ by

$$\theta_{N_1}=f^{(N_1)}(\tau_+)\ ,$$

and let $\beta=\beta_1(\alpha)$ be the locus of the pseudotrajectory RL^{N_1-1}—L, and $\beta=\beta_2(\alpha)$ the locus of the trajectory RL^{N_1-1}, so that

$$\theta_{N_1}(\beta=\beta_1)=\tau_-\ ,\quad \theta_{N_1}(\beta=\beta_2)=\tau_+\ .$$

Since

$$\frac{\partial f(\theta)}{\partial\beta}>0\ \text{ for }\ -\pi<\theta\le\tau_-\ \text{ or }\ \tau_+\le\theta\le\pi\ ,$$

we conclude that

$$\tau_-<\theta_{N_1}<\tau_+\ \text{ for }\ \beta_1<\beta<\beta_2$$

which means that the (N_1+1)th letter in the word of any trajectories of class 2 in the area A must be M. Thus these trajectories have words with prefix RL^{N_1-1}.

In the limit $\alpha\to\frac{1}{2}$ from above the middle piece of the map $f(\theta)$ becomes vertical and orbit words with prefix RL^{N_1-1} will reduce to a word RL^{N_1-1} exactly. Hence these trajectories terminate at the left end point of $[1/N_1]$. By similar considerations, we find that all the trajectories of class 1 in area C terminate at the right end point of $[1/N_1]$. On the other hand, in the area B no trajectories are present at all, and the stable orbit of the system has period N_1 when the parameters take values in this area. Derivations are immediate generalizations of the derivations for the [1/2] case, and are therefore omitted.

The series of pentagons based on (5.5) form the *first level* of our hierarchical description of the parameter space. The remaining part of parameter space consists of many triangular regions immediately above the gaps between each neighbor pair of intervals in (5.5), between $[1/(N_1+1)]$ and $[1/N_1]$, say. A group of trajectories of class 2 intersect the pseudotrajectory LRL^{N_1-1}—R and enter this triangle. On the other hand, a group of trajectories of class 1 intersect the pseudotrajectory RL^{N_1-1}—L and do also enter this triangle.

In order to discuss the second level of the structure, let us consider a series of mode-locking regions of the form $[1/(N_1+1/N_2)]$ between the intervals $[1/(N_1+1)]$ and $[1/N_1]$ at the line $\alpha=\frac{1}{2}$, for a given integer N_1. For $N_1=2$, e.g.,

$$[2/5],[3/7],\ldots,[(N_2-1)/(2N_2-1)],[N_2/(2N_2+1)],\ldots, \tag{5.6}$$

between [1/3] and [1/2]. Take any mode-locking region in (5.6), say $[N_2/(2N_2+1)]$. It follows from (3.8) that the left end point of $[N_2/(2N_2+1)]$ corresponds to a word $RL^2(RL)^{N_2-1}$ and its right end point to a word $L(RL)^{N_2}$. A pseudotrajectory with word $RL^2(RL)^{N_2-1}$—L starts from the left end point of $[N_2/(2N_2+1)]$ and a pseudotrajectory with word $L(RL)^{N_2}$—R starts from the right endpoint of $[N_2/(2N_2+1)]$. For each mode-locking region in (5.6) there are two such pseudotrajectories. Then we obtain a series of pentagons, sketched in Fig. 8(a). Derivations are immediate generalizations of the derivations for the first level, and are therefore omitted. The pentagon immediately above $[N_2/(2N_2+1)]$ is bounded by parts of the pseudotrajectories RL—L, $L(RL)^{N_2-1}$—R, $L(RL)^{N_2}$—R, $RL^2(RL)^{N_2-1}$—L, and by $[N_2/(2N_2+1)]$ itself. The collection of pentagons above all mode-locking regions $[1/(N_1+1/N_2)]$ belong to the *second level* of our hierarchical description.

A trajectory of class 1 with word $L(RL)^{N_2}$ and a trajectory of class 2 with word $RL^2(RL)^{N_2-1}$ divide the pentagon into three areas A, B, and C, shown in Fig. 8(b). By the same reasoning as above it is clear that all the trajectories of class 2 in area A have words with prefix $RL^2(RL)^{N_2-1}$, hence they must terminate at the left end point of $[N_2/(2N_2+1)]$. It is also quite clear that all the trajectories of class 1 in area C have words with prefix $L(RL)^{N_2}$, hence they must terminate at the right end point of $[N_2/(2N_2+1)]$. Again, no trajectories are present in the area B at all. The stable orbit of the system has a period $(2N_2+1)$ for parameters in this area.

This concludes the discussion of the second level in the

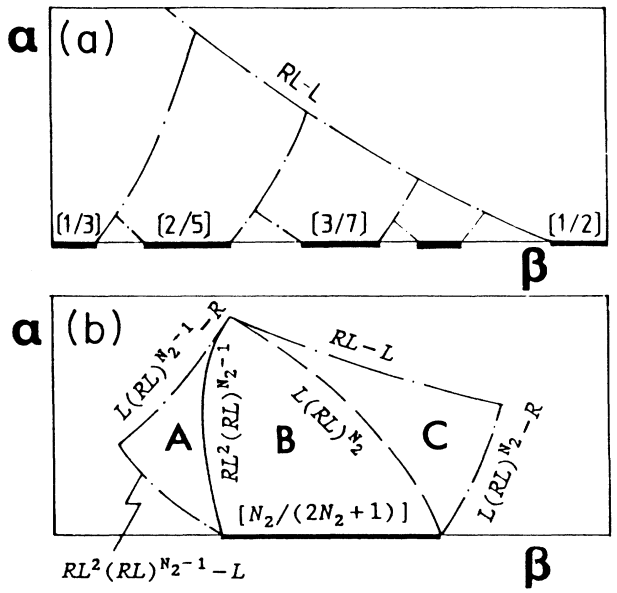

FIG. 8. (a) Pentagons connected to intervals of the second level (sketched only). (b) Blowup of the pentagon immediately above the interval $[N_2/(2N_2+1)]$.

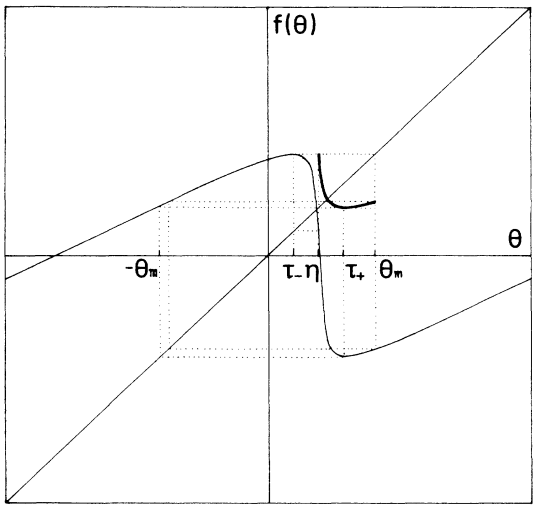

FIG. 9. The mapping (2.7) for $\alpha=0.52225$ and $\beta=0.40120$, parameter values on the pseudotrajectory $RLM-L$. The iteration (6.2) (the solid-heavy line) forms a unimodal mapping in the interval $[\eta,\theta_m]$.

parameter space. We may go on and discuss higher levels in the same way. At successive levels the words of the trajectories have longer and longer prefixes, and the pentagons become smaller and smaller in size. The set of pentagons corresponding to *all* intervals $[P/Q]$ will thereby be ordered in a hierarchy, and will fill the intermediate region of the parameter space (save a set of measure zero).

Coexistence of ordering of periodic orbits by the U sequence in strong-force situations and mode-locking behavior with rational winding numbers in weak-force situations has been noted before,[3,4,6], though the connection between them has apparently never been discussed. In the present model, the connection is exhibited in a systematic manner.

VI. NEW SEQUENCES OF PERIODIC ORBITS

As mentioned above, there are a lot of new sequences of periodic orbits in the intermediate region of parameter space, and their ordering may be different from both the U sequence and the Farey sequences. Since two classes of trajectories may intersect in the intermediate region, the stable state of the system may depend on the initial value.

The collection of all the trajectories in the parameter space can be subdivided into two families. Trajectories that start and end at the *same* end point of an interval $[P/Q]$ are called *closed-loop trajectories.* The remaining class we denote *Farey trajectories.* One can show that to any region $[P/Q]$ at least one period Q Farey trajectory of class 1 connects the right end point of $[P_a/Q_a]$ to that of $[P/Q]$, and one period Q Farey trajectory of class 2 connects the left end point of $[P/Q]$ to that of $[P_b/Q_b]$, where P_a/Q_a and P_b/Q_b are two consecutive fractions in a Farey series and $P/Q=(P_a+P_b)/(Q_a+Q_b)$ is their

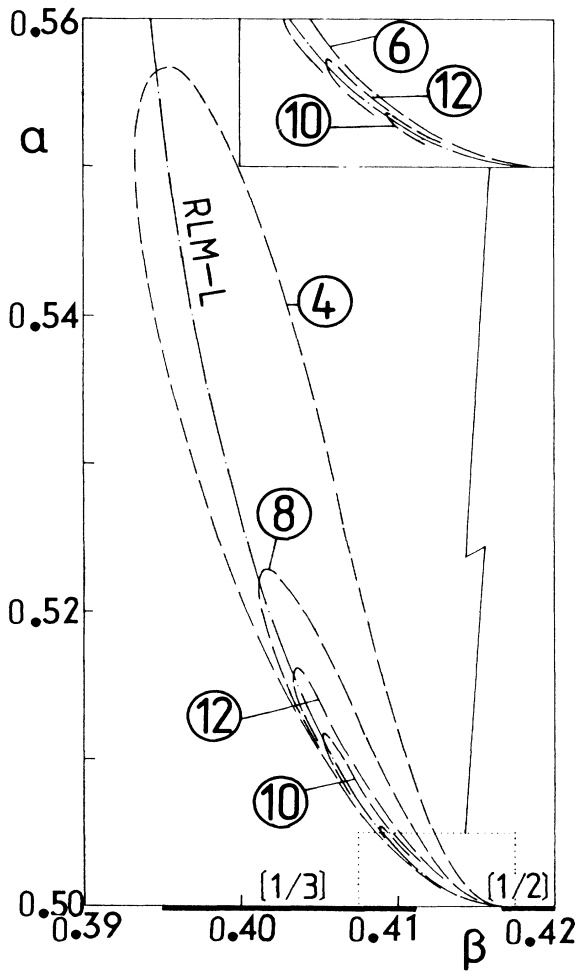

FIG. 10. A sequence of closed-loop trajectories of class 2 with parameter values along the pseudotrajectory $RLM-L$.

TABLE IV. A sequence of superstable orbits of class 2 along the pseudotrajectory $RLM-L$.

Order	Period[a]	β[b]	α[b]	Word
1	4	0.394 635 467 931	0.556 463 891 114	$RLML$
2	8	0.401 199 227 553	0.522 249 719 312	$RLMLRLML$
3	12	0.403 461 191 020	0.515 657 987 186	$RLMLRL(ML)^3$
4	10	0.405 389 607 636	0.511 271 720 827	$RLMLRL(ML)^2$
5	6	0.408 956 470 371	0.505 120 872 620	$RLMLRL$
6	12	0.410 396 245 423	0.503 383 538 693	$RLML(RL)^2MLRL$
7	10	0.412 210 589 092	0.501 720 435 699	$RLML(RL)^2ML$
8	12	0.413 744 462 240	0.500 761 998 276	$RLML(RL)^2(ML)^2$
9	8	0.414 598 934 301	0.500 374 235 418	$RRLML(RL)^2$
10	12	0.415 486 898 124	0.500 122 259 970	$RLML(RL)^3ML$
11	10	0.416 180 738 809	0.500 020 955 490	$RLML(RL)^3$
12	12	0.416 536 072 465	0.500 001 513 280	$RLML(RL)^4$

[a]Period ≤ 12 only.
[b]For superstable orbit.

mediant.[15] The proof is omitted here.

In the intermediate region we find a lot of new sequences of periodic orbits. The following are three examples.

(i) We have mentioned above that one can find the U sequence of class-1 trajectories along the pseudotrajectory $L-R$. Consider any one of them, say the trajectory with word $W=LRL^{N_1-2}X$, where X is a syllabus starting with M. The point of intersection between the pseudotrajectory $L-R$ and the trajectory $LRL^{N_1-2}X$ must be visited by the trajectory of class 2 with word $W'=RL^{N_1-2}XL$, which will terminate at the left end point of $[1/(N_1-1)]$ and form a closed-loop trajectory, since its word has prefix RL^{N_1-2}. If we keep the values of parameters α and β immediately below the pseudotrajectory $L-R$, and decrease β from $\frac{1}{2}$ to $\frac{1}{4}$, we will find a sequence of class-2 trajectories which is identical to the U sequence but every trajectory will be found twice. So the ordering of this sequence (with periods not longer than 6) should be

$$2,4,4,6,6,5,5,3,3,6,6,5,5,6,6,4,4,6,6,5,5,6,6\ . \quad (6.1)$$

Some of them are shown in Fig. 4(b). Notice that the first period-2 trajectory appears only once here because the other one is located in the $\beta > \frac{1}{2}$ region.

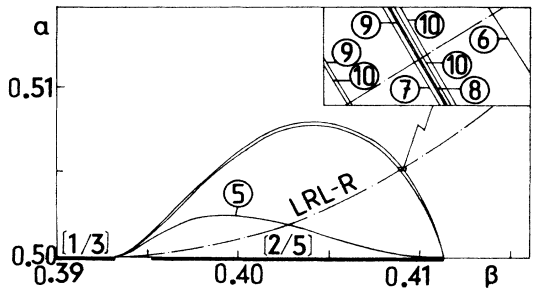

FIG. 11. A sequence of Farey trajectories of class 1 with parameter values along the pseudotrajectory $LRL-R$.

(ii) If the parameters α and β take values on the pseudotrajectory $RLM-L$, and η is defined as $f(-\theta_m)$, the successive iterations from τ_+ will be $-\theta_m$, η, and τ_-. It is clear that η must fall on branch M. Consider the iteration

$$\theta_{n+2}=F(\theta_n)\equiv f[f(\theta_n)] \quad (6.2)$$

on the interval $[\eta,\theta_m]$. It is not difficult to see that $F(\theta)$ is a unimodal mapping. In fact, the left part $\hat{R}$ of mapping $F(\theta)$, $\eta\leq\theta\leq\tau_+$, is constructed by two consecutive iterations of $f(\theta)$ on the branches M and L, and the right part $\hat{L}$ of $F(\theta)$, $\tau_+\leq\theta\leq\theta_m$, on the branches R and L, see Fig. 9. When the value of β increases along the pseudotrajectory $RLM-L$, a sequence of periodic orbits for the unimodal map (6.2) must result. Consequently the sequence of class-2 trajectories for superstable orbits with periods not longer than 12, should be ordered as

$$4,8,12,10,6,12,10,12,8,12,10,12\ . \quad (6.3)$$

These closed-loop trajectories start and end at the left end point of the interval [1/2], see Fig. 10. Their words can be obtained from the words in the U sequence based upon $F(\theta)$ by changing the letter $\hat{R}$ to ML and $\hat{L}$ to RL. With the values of α and β along this pseudotrajectory one

TABLE V. A sequence of superstable orbits of class 1 along the pseudotrajectory $LRL-R$.

Order	Period[a]	β[b]	Word
1	6	0.408 884 212 698	$LRLMLM$
2	10	0.408 755 319 598	$LRLMLM^2RLM$
3	10	0.408 754 098 280	$LRLMLM^3LM$
4	8	0.408 752 174 027	$LRLMLM^3$
5	10	0.408 752 146 853	$LRLMLM^5$
6	9	0.408 752 146 453	$LRLMLM^4$
7	7	0.408 750 273 861	$LRLMLM^2$
8	9	0.408 632 061 939	$LRLMLM^2LM$
9	10	0.408 621 172 806	$LRLMLM^2LM^2$
10	5	0.402 696 927 368	$LRLML$

[a]Period ≤ 10 only.
[b]For superstable orbit.

TABLE VI. A sequence of period-doubling bifurcations along the pseudotrajectory $LRL-R$. The β values for the superstable orbits and the corresponding Feigenbaum convergence rate δ (calculated as a ratio of two successive β intervals) are shown.

Order	Period	β	δ
1	16	0.408 884 212 697 52	
2	12	0.408 793 374 733 54	
3	24	0.408 784 834 029 06	10.6359
4	48	0.408 783 695 052 33	7.4986
5	96	0.408 783 499 023 57	5.8103
6	192	0.408 783 458 686 70	4.8598
7	384	0.408 783 450 108 57	4.7023
8	768	0.408 783 448 274 04	4.6759
9	1536	0.408 783 447 881 26	4.6706
10	3072	0.408 783 447 797 14	4.6694

finds the series of superstable orbits (6.3). The results for the corresponding values of β and the symbolic dynamics words are given in Table IV. Notice that all these orbits have words with prefix RL. The Feigenbaum convergence rate for period-doubling bifurcations should be $\delta=7.284\ldots$, representative for unimodal mappings with a fourth-order maximum.

(iii) Another example is a sequence of class-1 trajectories, corresponding to a series of superstable orbits with period

$$6,10,10,8,10,9,7,9,10,5,\ldots, \tag{6.4}$$

connecting the right end points of two intervals [1/3] and [2/5], see Fig. 11. All of these Farey trajectories intersect the pseudotrajectory $LRL-R$, which can be well approximated by

$$\alpha=0.5+20.3(\beta-\tfrac{11}{28})^2 . \tag{6.5}$$

The formula (6.5) is obtained numerically. Along the curve (6.5) one finds the series (6.4) of superstable orbits. The results for the corresponding parameter values and words are shown in Table V. We can give a proof (not reproduced here) that along the pseudotrajectory $LRL-R$ every trajectory of class 1, which is located between the pseudotrajectories $RLM-L$ and $RL-L$ and corresponds to superstable orbits with periods not longer than 10, is included in (6.4).

Moreover, from these periodic orbits one can also find period-doubling bifurcations with the usual Feigenbaum convergence rate,[16] $\delta=4.6692\ldots$. For example, from the orbit with period 6, the first one in (6.4), the sequence of period-doubling bifurcations is shown in Table VI.

It is quite obvious that the examples given above belong neither to the U sequence nor to the Farey sequence. While the systematics of the (6.1) and (6.3) has been clarified above, the systematics of the series (6.4) of superstable orbits is not clear for longer periods. We conclude by noting that although we have made a systematic connection between the unimodal strong force situation and the mode-locking weak force region through the intermediate region, the latter contains an interesting and complicated fine structure that remains to be unraveled.

ACKNOWLEDGMENTS

The author wishes to thank the Trondheim Institute of Theoretical Physics for its hospitality, and especially to thank Professor P. C. Hemmer for helpful discussions, continual encouragements and critical reading of the manuscript. The author is also grateful to the Royal Norwegian Council for Scientific and Industrial Research (NTNF) for financial support.

APPENDIX

In this appendix we will prove theorem 1. The proof is based on the following lemma.[14]

Lemma 1. Let $w=P/Q$ with $0<P<Q$. Then the word corresponding to the left end point of the interval $[P/Q]$ is

$$W=A_0A_1\cdots A_k\cdots A_{Q-1} , \tag{A1}$$

with

$$A_k=\begin{cases} R & \text{if } \Delta(k)=1 , \\ L & \text{if } \Delta(k)=0 , \end{cases}$$

where

$$\Delta(k)=[kP/Q]-[(k-1)P/Q] , \quad 0\le k<Q . \tag{A2}$$

Here $[x]$ denotes the integer part of x. $\Delta(k)$ is clearly 0 or 1, since $kP/Q-(k-1)P/Q=P/Q<1$.

The above result has been deduced in Ref. 14, so we will not repeat the proof here. A more convenient expression is contained in the following lemma.

Lemma 2. The word (A1) can be written as

$$W=RL^{l_1(0)}RL^{l_1(1)}\cdots RL^{l_1(k_1)}\cdots RL^{l_1(P-1)} , \tag{A3}$$

where

$$l_1(k_1)=\{(k_1+1)Q/P\}-\{k_1Q/P\}-1 , \quad 0\le k_1<P . \tag{A4}$$

Here $\{x\}$ denotes the smallest integer not less than x.

Proof. Denoting such k which make $\Delta(k)=1$ by k^*, we have that to each k^* corresponds an integer $k_1=[k^*P/Q]$ such that $k^*P/Q\ge k_1>(k^*-1)P/Q$. So $k^*\ge k_1Q/P>k^*-1$, i.e.,

$$k^*=k^*(k_1)=\{k_1Q/P\} . \tag{A5}$$

Here $0\le k_1<P$, since $0\le k<Q$. An R occurs whenever k_1 increases (by unity). Hence the number of letters L between two consecutive R's must be $l_1(k_1)=k^*(k_1+1)-k^*(k_1)-1$, and the formulas (A3) and (A4) are then obtained.

Corollary 1. Corresponding to the winding number

$$w_1=\frac{1}{N_1} ,$$

the word is

$$W_1=RL^{N_1-1} . \tag{A6}$$

Putting $P=1$ and $Q=N_1$ in lemma 2 we find that k_1 must be 0, and $l_1(0)=N_1-1$. The formula (A6) is then

obtained.

Definition. For a given winding number

$$w=\frac{P}{Q}=\cfrac{1}{N_1+\cfrac{1}{N_2+\cdots}}$$

the sequence of integers S_j $(j\geq 2)$ is defined by

$$\begin{aligned} &S_2=Q-N_1P\ ,\\ &S_3=P-N_2S_2\ ,\\ &S_4=S_2-N_3S_3\ ,\\ &\vdots\\ &S_{j+2}=S_j-N_{j+1}S_{j+1}\ . \end{aligned} \tag{A7}$$

Lemma 3. Let

$$w=\frac{P}{Q}=\cfrac{1}{N_1+\cfrac{S_2}{P}}\ ,\quad 0<S_2<P\ . \tag{A8}$$

Then the corresponding word is

$$\begin{aligned} W=&(W_1LW_1^{l_2(0)})(W_1LW_1^{l_2(1)})\\ &\cdots(W_1LW_1^{l_2(k_2)})\cdots(W_1LW_1^{l_2(S_2-1)})\ , \end{aligned} \tag{A9}$$

where W_1 is given by (A6), and with

$$l_2(k_2)=[(k_2+1)P/S_2]-[k_2P/S_2]-1\ ,\quad 0\leq k_2<S_2\ . \tag{A10}$$

Proof. It follows from (A4) and (A7) that $l_1(k_1)=(N_1-1)+\Delta_1(k_1)$, where

$$\Delta_1(k_1)=\{(k_1+1)S_2/P\}-\{k_1S_2/P\}\ . \tag{A11}$$

$\Delta_1(k_1)$ must be 1 or 0, since $(k_1+1)S_2/P-k_1S_2/P=S_2/P<1$. Denoting such k_1 which make $\Delta_1(k_1)=1$ for k_1^*, we have that each k_1^* corresponds to an integer k_2 such that $(k_1^*+1)S_2/P>k_2\geq k_1^*S_2/P$. So $k_1^*+1>k_2P/S_2\geq k_1^*$, i.e.,

$$k_1^*=k_1^*(k_2)=[k_2P/S_2]\ . \tag{A12}$$

Here $0\leq k_2<S_2$, since $0\leq k_1<P$. The formula (A4) then becomes

$$l_1(k_1)=\begin{cases}N_1 & \text{if } k_1=k_1^*\\ N_1-1 & \text{if } k_1\neq k_1^*\ .\end{cases}$$

The number of syllables $RL^{N_1-1}=W_1$ between two consecutive $RL^{N_1}=W_1L$ must be $l_2(k_2)=k_1^*(k_2+1)-k_1^*(k_2)-1$, and the formulas (A9) and (A10) are then obtained.

Corollary 2. Corresponding to the winding number

$$w_2=\cfrac{1}{N_1+\cfrac{1}{N_2}}\ ,$$

the word is

$$W_2=W_1LW_1^{N_2-1}\ . \tag{A13}$$

Putting $S_2=1$ and $P=N_2$ in the lemma 3 we find that k_2 must be 0, and $l_2(0)=N_2-1$. Corollary 2 then results.

Lemma 4. Let

$$w=\frac{P}{Q}=\cfrac{1}{N_1+\cfrac{1}{N_2+\cfrac{S_3}{S_2}}}\ ,\quad 0<S_3<S_2\ .$$

Then the corresponding word is

$$\begin{aligned} W=&(W_2^{l_3(1)}W_1)(W_2^{l_3(2)}W_1)\\ &\cdots(W_2^{l_3(k_3)}W_1)\cdots(W_2^{l_3(S_3)}W_1)\ , \end{aligned} \tag{A14}$$

where W_1 and W_2 are defined above, and where

$$l_3(k_3)=\{k_3S_2/S_3\}-\{(k_3-1)S_2/S_3\}\ ,\quad 0<k_3\leq S_3\ . \tag{A15}$$

Proof. It is clear from (A10) and (A7) that $l_2(k_2)=(N_2-1)+\Delta_2(k_2)$, where

$$\Delta_2(k_2)=[(k_2+1)S_3/S_2]-[k_2S_3/S_2]\ . \tag{A16}$$

$\Delta_2(k_2)$ must be 1 or 0, since $(k_2+1)S_3/S_2-k_2S_3/S_2=S_3/S_2<1$. Denoting such k_2 which make $\Delta_2(k_2)=1$ for k_2^*, we have that each k_2^* corresponds to an integer k_3 such that $(k_2^*+1)S_3/S_2\geq k_3>k_2^*S_3/S_2$. So $k_2^*+1\geq k_3S_2/S_3>k_2^*$, i.e.,

$$k_2^*=k_2^*(k_3)=\{k_3S_2/S_3\}-1\ . \tag{A17}$$

Here $0<k_3\leq S_3$, since $0\leq k_2<S_2$. The formula (A10) then becomes

$$l_2(k_2)=\begin{cases}N_2 & \text{if } k_2=k_2^*\ ,\\ N_2-1 & \text{if } k_2\neq k_2^*\ .\end{cases}$$

The number of syllables $W_1LW_1^{N_2-1}=W_2$ before the first $W_1LW_1^{N_2}$, or between two consecutive $W_1LW_1^{N_2}=W_2W_1$, must be $k_2^*(k_3)-k_2^*(k_3-1)-1$, and the formulas (A14) and (A15) are then obtained.

Corollary 3. Corresponding to the winding number

$$w_3=\cfrac{1}{N_1+\cfrac{1}{N_2+\cfrac{1}{N_3}}}\ ,$$

the word is

$$W_3=W_2^{N_3}W_1\ . \tag{A18}$$

Proof by putting $S_3=1$ and $S_2=N_3$ in lemma 4 which gives $k_3=1$ and $l_3(1)=N_3$.

Lemma 5. Let

$$w=\frac{P}{Q}=\cfrac{1}{N_1+\cfrac{1}{N_2+\cfrac{1}{N_3+\cfrac{S_4}{S_3}}}}\ ,\quad 0<S_4<S_3\ .$$

Then the corresponding word is

$$W=(W_2W_3^{l_4(0)})(W_2W_3^{l_4(1)})\cdots(W_2W_3^{l_4(k_4)})\cdots(W_2W_3^{l_4(S_4-1)}), \tag{A19}$$

where

$$l_4(k_4)=[(k_4+1)S_3/S_4]-[k_4S_3/S_4],\quad 0\le k_4<S_4. \tag{A20}$$

Proof. From (A15) and (A7) follows that $l_3(k_3)=N_3+\Delta_3(k_3)$, where

$$\Delta_3(k_3)=\{k_3S_4/S_3\}-\{(k_3-1)S_4/S_3\}. \tag{A21}$$

$\Delta_3(k_3)$ is 1 or 0, since $k_3S_4/S_2-(k_3-1)S_4/S_3=S_4/S_3<1$. Denoting such k_3 which make $\Delta_3(k_3)=1$ for k_3^*, we have that each k_3^* corresponds to an integer k_4 such that $k_3^*S_4/S_3>k_4\ge(k_3^*-1)S_4/S_3$. So $k_3^*>k_4S_3/S_4\ge k_3^*-1$, i.e.,

$$k_3^*=k_3^*(k_4)=[k_4S_3/S_4]+1. \tag{A22}$$

Here $0\le k_4<S_4$, since $0<k_3\le S_3$. The formula (A15) then becomes

$$l_3(k_3)=\begin{cases}N_3+1 & \text{if } k_3=k_3^*,\\ N_3 & \text{if } k_3\ne k_3^*.\end{cases}$$

The number of syllables $W_2^{N_3}W_1=W_3$ between two nearest $W_2^{N_3+1}W_1=W_2W_3$ must be $k_3^*(k_4+1)-k_3^*(k_4)-1$, and the formulas (A19) and (A20) are then obtained.

Corollary 4. Corresponding to the winding number

$$w_4=\cfrac{1}{N_1+\cfrac{1}{N_2+\cfrac{1}{N_3+\cfrac{1}{N_4}}}},$$

the word is

$$W_4=W_2W_3^{N_4}. \tag{A23}$$

Putting $S_4=1$ and $S_3=N_4$ in lemma 5 we find that k_4 must be 0, and $l_4(0)=N_4$. The corollary 4 is then obtained.

Now we shall prove the theorem 1 by induction. The theorem has already been shown to be valid for $j\le 4$.

In case j is odd, we make the induction assumption that for $j=2n$ $(n\ge 2)$ the winding number

$$w=\frac{P}{Q}=\cfrac{1}{N_1+\cfrac{1}{N_2+\cdots+\cfrac{1}{N_{2n-1}+\cfrac{S_{2n}}{S_{2n-1}}}}},\quad 0<S_{2n}<S_{2n-1}$$

corresponds to the word

$$W=(W_{2n-2}W_{2n-1}^{l_{2n}(0)})(W_{2n-2}W_{2n-1}^{l_{2n}(1)})\cdots(W_{2n-2}W_{2n-1}^{l_{2n}(k_{2n})})\cdots(W_{2n-2}W_{2n-1}^{l_{2n}(S_{2n}-1)}), \tag{A24}$$

where

$$l_{2n}(k_{2n})=[(k_{2n}+1)S_{2n-1}/S_{2n}]-[k_{2n}S_{2n-1}/S_{2n}],\quad 0\le k_{2n}<S_{2n}. \tag{A25}$$

As a consequence the word corresponding to $j=2n$ is

$$W_{2n}=W_{2n-2}W_{2n-1}^{N_{2n}}, \tag{A26}$$

in accordance with theorem 1.

It is easy to deduce from (A25) and (A7) that $l_{2n}(k_{2n})=N_{2n}+\Delta_{2n}(k_{2n})$, where

$$\Delta_{2n}(k_{2n})=[(k_{2n+1})S_{2n+1}/S_{2n}]-[k_{2n}S_{2n+1}/S_{2n}]. \tag{A27}$$

$\Delta_{2n}(k_{2n})$ must be 1 or 0, since $(k_{2n}+1)S_{2n+1}/S_{2n}-k_{2n}S_{2n+1}/S_{2n}=S_{2n+1}/S_{2n}<1$. Denoting such k_{2n} which make $\Delta_{2n}(k_{2n})=1$ for k_{2n}^*, we have that each k_{2n}^* corresponds to an integer k_{2n+1} such that $(k_{2n}^*+1)S_{2n+1}/S_{2n}\ge k_{2n+1}>k_{2n}^*S_{2n+1}/S_{2n}$. So $k_{2n}^*+1\ge k_{2n+1}S_{2n}/S_{2n+1}>k_{2n}^*$, i.e.,

$$k_{2n}^*=k_{2n}^*(k_{2n+1})=\{k_{2n+1}S_{2n}/S_{2n+1}\}-1. \tag{A28}$$

Here $0<k_{2n+1}\le S_{2n+1}$, since $0\le k_{2n}<S_{2n}$. The formula (A25) then becomes

$$l_{2n}(k_{2n})=\begin{cases}N_{2n}+1 & \text{if } k_{2n}=k_{2n}^*,\\ N_{2n} & \text{if } k_{2n}\ne k_{2n}^*.\end{cases}$$

The number of syllables $W_{2n-2}W_{2n-1}^{N_{2n}}=W_{2n}$ between two nearest $W_{2n-2}W_{2n-1}^{N_{2n}+1}=W_{2n}W_{2n-1}$ must be $l_{2n+1}(k_{2n+1})=k_{2n}^*(k_{2n+1})-k_{2n}^*(k_{2n+1}-1)-1$, and then we obtain

$$W=(W_{2n}^{l_{2n+1}(1)}W_{2n-1})(W_{2n}^{l_{2n+1}(2)}W_{2n-1})\cdots(W_{2n}^{l_{2n+1}(k_{2n}+1)}W_{2n-1})\cdots(W_{2n}^{l_{2n+1}(S_{2n+1})}W_{2n-1}) , \tag{A29}$$

with

$$l_{2n+1}(k_{2n+1})=\{k_{2n+1}S_{2n}/S_{2n+1}\}-\{(k_{2n+1}-1)S_{2n}/S_{2n+1}\} , \quad 0<k_{2n+1}\leq S_{2n+1} , \tag{A30}$$

and, in particular, that

$$W_{2n+1}=W_{2n}^{N_{2n+1}}W_{2n-1} . \tag{A31}$$

Hence the theorem holds for odd j, which completes this part of the induction proof. It remains to consider j even. Equations (A29), (A30), and (A31) are useful to prove the theorem for even j. This part of the proof is omitted here, since it is very similar to that case where j is odd.

---

*On leave from the Institute of Low-Energy Nuclear Physics, Beijing Normal University, Beijing, China.

[1]B. A. Hubermann and J. D. Crutchfield, Phys. Rev. Lett. **43**, 1743 (1979).
[2]J. B. McLaughlin, J. Stat. Phys. **24**, 375 (1981).
[3]B. L. Hao and S. Y. Zhang, J. Stat. Phys. **28**, 769 (1982).
[4]B. L. Hao, G. R. Wang, and S. Y. Zhang, Commun. Theor. Phys. **2**, 1075 (1983).
[5]R. Räty, J. von Boehm, and H. M. Isomäki, Phys. Lett. **103A**, 289 (1984).
[6]D. L. Gonzalez and D. Piro, Phys. Rev. Lett. **50**, 870 (1983); Phys. Lett. **101A**, 455 (1984).
[7]H. M. Isomäki, J. von Boehm, and R. Räty, Phys. Lett. **107A**, 343 (1985).
[8]B. L. Hao, *Chaos* (World Scientific, Singapore, 1984).
[9]E. J. Ding (unpublished).
[10]M. H. Jensen, P. Bak, and T. Bohr, Phys. Rev. Lett. **50**, 1637 (1983); Phys. Rev. A **30**, 1960 (1984), and references therein.
[11]L. Glass and R. Perez, Phys. Rev. Lett. **48**, 1772 (1982).
[12]E. J. Ding, Phys. Rev. A **34**, 3547 (1986).
[13]N. Metropolis, M. L. Stein, and P. R. Stein, J. Comb. Theor. Ser. A **15**, 25 (1973).
[14]E. J. Ding and P. C. Hemmer, J. Stat. Phys. **46**, 99 (1987).
[15]W. J. LeVeque, *Topics in Number Theory* (Addison-Wesley, Reading, Mass., 1956), Vol. 1; L. E. Dickson, *Theory of Numbers* (Chelsea, New York, 1966), Vol. 1.
[16]M. J. Feigenbaum, J. Stat. Phys. **19**, 25 (1978); **21**, 669 (1979).
[17]R. V. Mendes, Phys. Lett. **84A**, 1 (1981).